



Article

Upper Ocean Responses to the Tropical Cyclones Ida and Felicia (2021) in the Gulf of Mexico and the Eastern North Pacific

Sebastian Neun [†] , Jan Jacob [†] and Oliver Wurl ^{*†} Institute for Chemistry and Biology of the Marine Environment, University of Oldenburg,
26382 Wilhelmshaven, Germany

* Correspondence: oliver.wurl@uni-oldenburg.de

† These authors contributed equally to this work.

Abstract: Tropical cyclones (TCs) are a significant component of ocean–atmosphere interactions and the climate system. These interactions determine both the development and strength of TCs, as well as various biogeochemical processes in the upper oceans, including vertical mixing and primary production. We investigated the impact of the TCs Felicia and Ida that emerged in 2021 in the eastern North Pacific and the Gulf of Mexico, respectively, using satellite observations of sea-surface temperature (SST) and surface chlorophyll a (chl-a) concentrations, and vertical profiles of temperature and salinity derived from Argo floats. Observations differed between the two study areas. Cooling of SST associated with TC Ida was observed throughout the Gulf of Mexico (<0.5 °C), except for warming in a region off the Mexican coast east of Ida’s track (by about 0.5 °C). The passing of TC Felicia cooled SST in the eastern region (15°N, 115°W) and a central region (15°N, 125°W) by 0.5 °C and 0.36 °C, respectively. The passing of the TCs caused enhanced vertical mixing of the upper ocean layer in the Gulf of Mexico, with a deepening of the mixed layers from 38 m to 68 m (TC Ida). In contrast, the mixed layer in the eastern North Pacific decreased from 50 m to 20 m. For the eastern North Pacific, mixing could be related to an increase in surface chl-a and thus enhanced phytoplankton biomass was observed for 2 months after the passing of TC Felicia with a chl-a increase of 0.15 mg m⁻³. In the Gulf of Mexico, however, TC Ida caused the injection of a coastal phytoplankton bloom into the open Gulf, resting for more than a month after the cyclone had passed. Our findings contribute to the understanding of potential SST cooling, destratification, and enhanced primary production due to the passage of TCs in two distinct ocean regions, i.e., the open eastern North Pacific and the semi-enclosed Gulf of Mexico.



Citation: Neun, S.; Jacob, J.; Wurl, O. Upper Ocean Responses to the Tropical Cyclones Ida and Felicia (2021) in the Gulf of Mexico and the Eastern North Pacific. *Remote Sens.* **2022**, *14*, 5520. <https://doi.org/10.3390/rs14215520>

Academic Editors: Korak Saha and Zhankun Wang

Received: 26 September 2022

Accepted: 1 November 2022

Published: 2 November 2022

Publisher’s Note: MDPI stays neutral with regard to jurisdictional claims in published maps and institutional affiliations.



Copyright: © 2022 by the authors. Licensee MDPI, Basel, Switzerland. This article is an open access article distributed under the terms and conditions of the Creative Commons Attribution (CC BY) license (<https://creativecommons.org/licenses/by/4.0/>).

Keywords: tropical cyclone; SST; Argo; chlorophyll a; Gulf of Mexico; eastern North Pacific

1. Introduction

Tropical cyclones (TCs) pose a significant threat to the lives of humans along coastlines, infrastructures, and ecosystems. The global frequency of TCs has remained consistent, but there can be substantial inter-annual to multi-decadal variability in frequency and strength within individual ocean basins [1]. These variabilities challenge scientists to determine disaster planning for severely affected regions. In recent decades, research has focused on a mechanistic understanding of the formation of TCs and the prediction of tracks and landfalls. Overall, the evolution, behavior, and destructiveness of TCs are fundamentally coupled to the characteristics and interactions between the atmosphere, ocean, and land masses [2–4]. TCs typically develop from a pre-existing atmospheric disturbance and require a number of conditions, including SST above 26 °C, low vertical wind shear, humid air, and Coriolis force, to intensify and fully develop into a cyclonic vortex (e.g., [2,5,6]). These conditions are met in both hemispheres between latitudes 5° and 30°.

Despite their destructive nature, TCs have a significant impact on biogeochemical processes in the upper ocean. Cooling of SST and an increase in phytoplankton biomass

are the most frequently reported responses of the upper ocean after the passage of a TC [7]. Cooling in SST is caused by strong vertical mixing and upward entrainment of deeper, colder water due to intense TC winds rather than by the exchange of latent and sensible heat with the atmosphere [3,8,9]. Hence, slow-moving TCs that act longer on the upper ocean layer induce greater cooling [3,10]. The amplitude of SST cooling also depends on the pre-existing water column stratification. Whereas the mixing of a strongly temperature-stratified water column provides negative feedback to TC intensity because of the aforementioned SST cooling [4,11,12], salinity-induced barrier layers inhibit vertical mixing, thereby allowing TCs to further intensify [13]. Thus, the strongest cyclones develop most frequently in areas where ocean pre-conditions inhibit pronounced cooling [11,12,14].

In addition to the cooling of SST, the surface chlorophyll-a (chl-a) concentration typically increases after the passage of a TC, as can be observed from satellite imagery. This enhancement of chl-a can arise either from the upward entrainment of phytoplankton from the deeper chlorophyll maximum or from new production [15–17]. After a TC, the new production of phytoplankton is fueled by the upward transport of colder, nutrient-enriched deeper water [15,17,18] or, in near-shore regions, by resuspension and increased terrestrial runoff [19–21]. This biological response is typically observed 3–6 days after the passage of a TC but can last for 2–3 weeks [15,20,22]. Enhancement of chl-a concentration by TCs has far-reaching effects on marine biogeochemical processes and contributes, for example, to the interannual variability in primary production in the western subtropical North Atlantic [23].

TCs in the eastern North Pacific are of particular interest as they are the second most common in the world [24], but have received relatively little scientific attention in the past. However, more recent literature indicates diverse forcings in TC formation in the eastern North Pacific including El Niño [25], mountain ranges across North America [26], monsoon seasons [24,27] and location of the inter-tropical convergence zone [27]. For this reason, it is of particular interest to fill gaps in the understanding of TCs in the eastern North Pacific in comparison to the western North Pacific and North Atlantic. That should also include the response of the upper ocean due to the relevance of ocean mixing and primary productivity.

To further elucidate the region-specific impacts of TCs on SST and chl-a, this study focused on two TCs that emerged in 2021 in the Gulf of Mexico (TC Ida) and the eastern North Pacific (TC Felicia). Both TCs were classified as category 4 hurricanes according to the Saffir-Simpson Hurricane Wind Scale but occurred in completely different regions: a semi-enclosed ocean basin (Gulf of Mexico) and an open ocean (eastern North Pacific). Nearly concomitant with TC Felicia, the tropical storm Guillermo formed further north in the eastern North Pacific. We analyzed the potential joint impacts of Felicia and Guillermo on the upper ocean and investigated their effects on SST, vertical profiles of temperature and salinity derived from Argo floats, and surface chl-a concentration.

2. Materials and Methods

2.1. Study Area

TC Ida developed in the Caribbean Sea on 26 August 2021 and proceeded toward the Gulf of Mexico. At that point, Ida reached wind speeds up to 240 km h^{-1} before it finally made landfall on 29 August 2021 close to New Orleans, USA, and passed over the states of Louisiana and Mississippi [28]. The eye of the TC was around 27.8 km wide during landfall [28]. Ida was the strongest TC to pass over the Gulf of Mexico in 2021 and became the fifth costliest hurricane on record [28].

In the eastern North Pacific, TC Felicia developed as a compact cyclone with no damage or casualties [29]. TC Felicia developed as a tropical depression near the south-southwestern coast of Mexico on 14 July 2021 and reached its peak intensity on 17 July 2021, with wind speeds of up to 230 km h^{-1} [29]. Strong winds, however, extended only up to 28 km from the eye, indicating that Felicia was a relatively small-scale TC. Moving westward, Felicia finally dissipated on 22 July 2021 over waters with temperatures below $26 \text{ }^{\circ}\text{C}$ and strong wind shear, approximately 1000 km southeast of the Hawaiian Islands [29].

Three days after the development of Felicia (i.e., 17 July 2021), the storm Guillermo developed south-southwest of Mexico. Guillermo was a short-lived tropical storm with maximum wind speeds of 93 km h^{-1} and a track nearly parallel to that of Felicia, located approximately 400–450 km north [30]. Increasing wind shear and movement over cold waters below $26 \text{ }^\circ\text{C}$ caused Guillermo to weaken, so it dissipated four days after development on 21 July 2021 [30].

Along the tracks of the TCs, different regions of interest were predefined to specifically look at the extent of anomalies of SST and surface chl-a concentration. For TC Ida, the Gulf of Mexico was divided into five different regions to study changes in SST. These were called “Gulf of Mexico (GoM),” encompassing the whole basin; “Houston Area (HA),” a coastal region south of the city of Houston, Texas; “West Florida (WF),” a coastal region along the west coast of the state of Florida; “Central Basin (CB),” a region north of Cuba and the Yucatán peninsula; and “Offshore Mexico (OM),” overlapping with the Bay of Campeche in the south of the Gulf of Mexico. For surface chl-a anomalies, only a region west of Florida was analyzed. The regions are indicated in Figures 1A and 2.

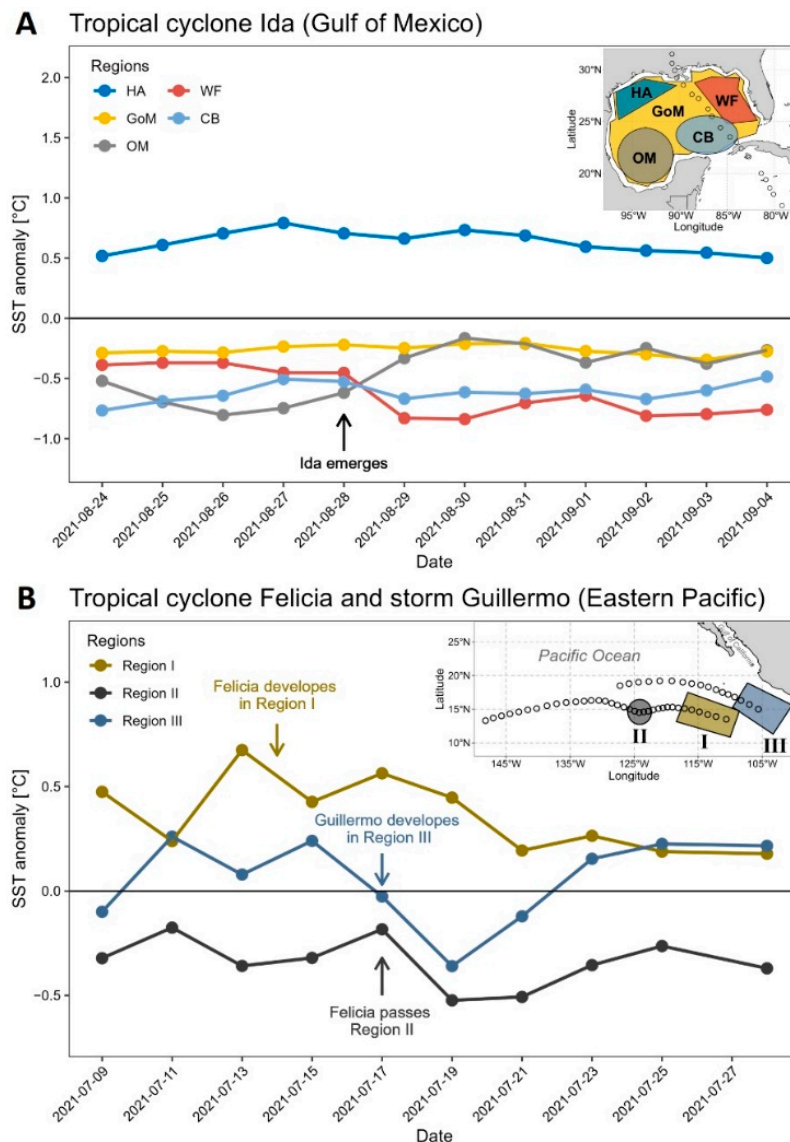


Figure 1. Anomalies in SST related to Ida (A) and Felicia and Guillermo (B) for the respective regions of interest. Days when the storm develops or passes are indicated by arrows and described in the panels.

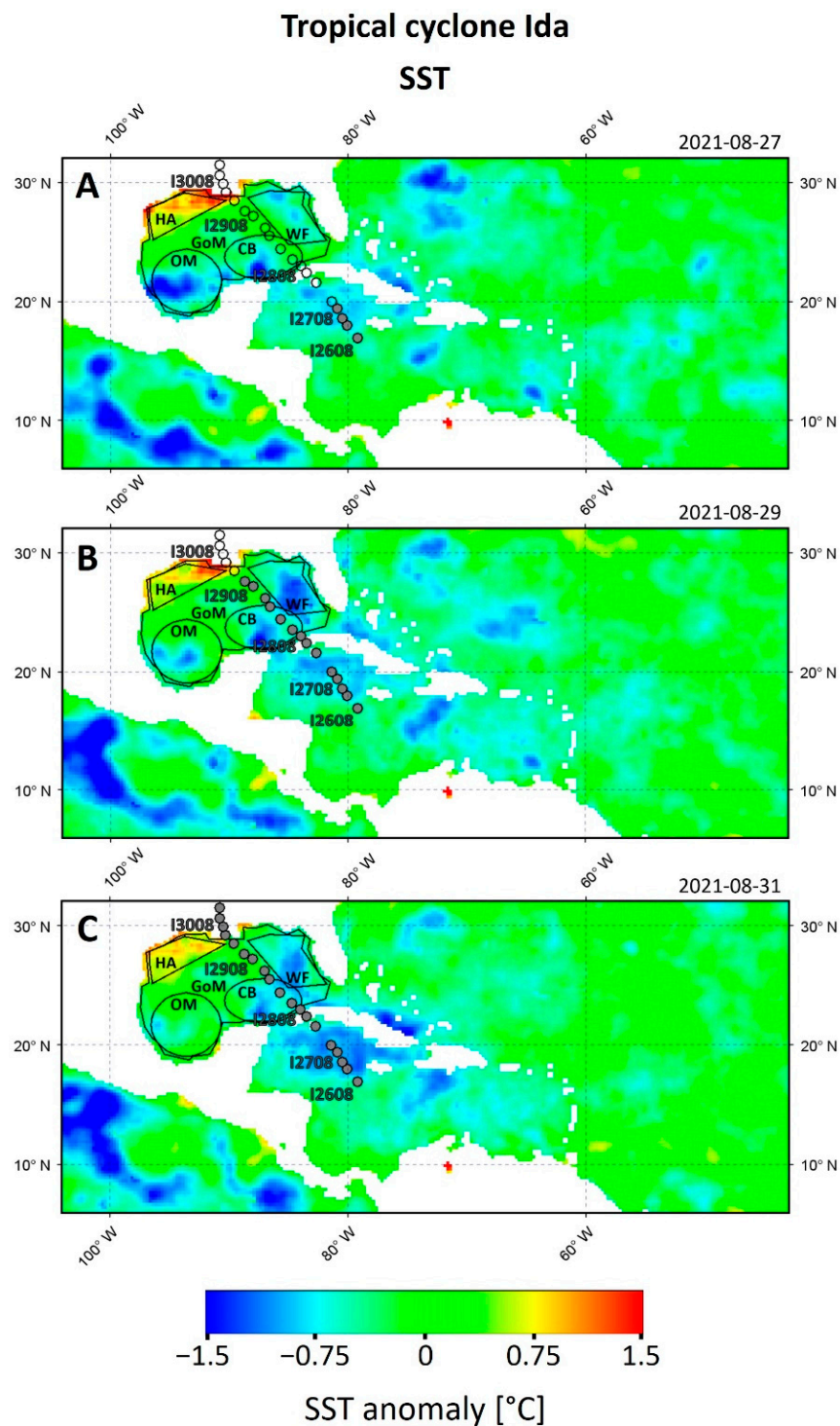


Figure 2. Anomaly maps for SST in the study area of TC Ida for (A) 27 August 2021, (B) 29 August 2021 and (C) 31 August 2021. Anomalies are color-coded as indicated by the color bar. Tracks are marked with circles, where open circles indicate that the storm has not yet passed the position yet. The labels along the track indicate position of Ida (I) on a particular day and month, e.g., I2608. The dates of the satellite images are given in the top right of each panel. White space indicates areas without data.

For TC Felicia and tropical storm Guillermo in the eastern North Pacific, three regions of interest were defined to examine anomalies in SST and surface chl-a. Regions that represent the places of origin of Felicia and Guillermo were examined and referred to as “Region I” (origin of Felicia) and “Region III” (origin of Guillermo). We defined a third

region that overlapped (for SST) or was located south of the position (for surface chl-a), where Felicia reached maximum wind speeds as TC. This region is referred to as “Region II.” The defined regions are shown in Figures 1B and 3.

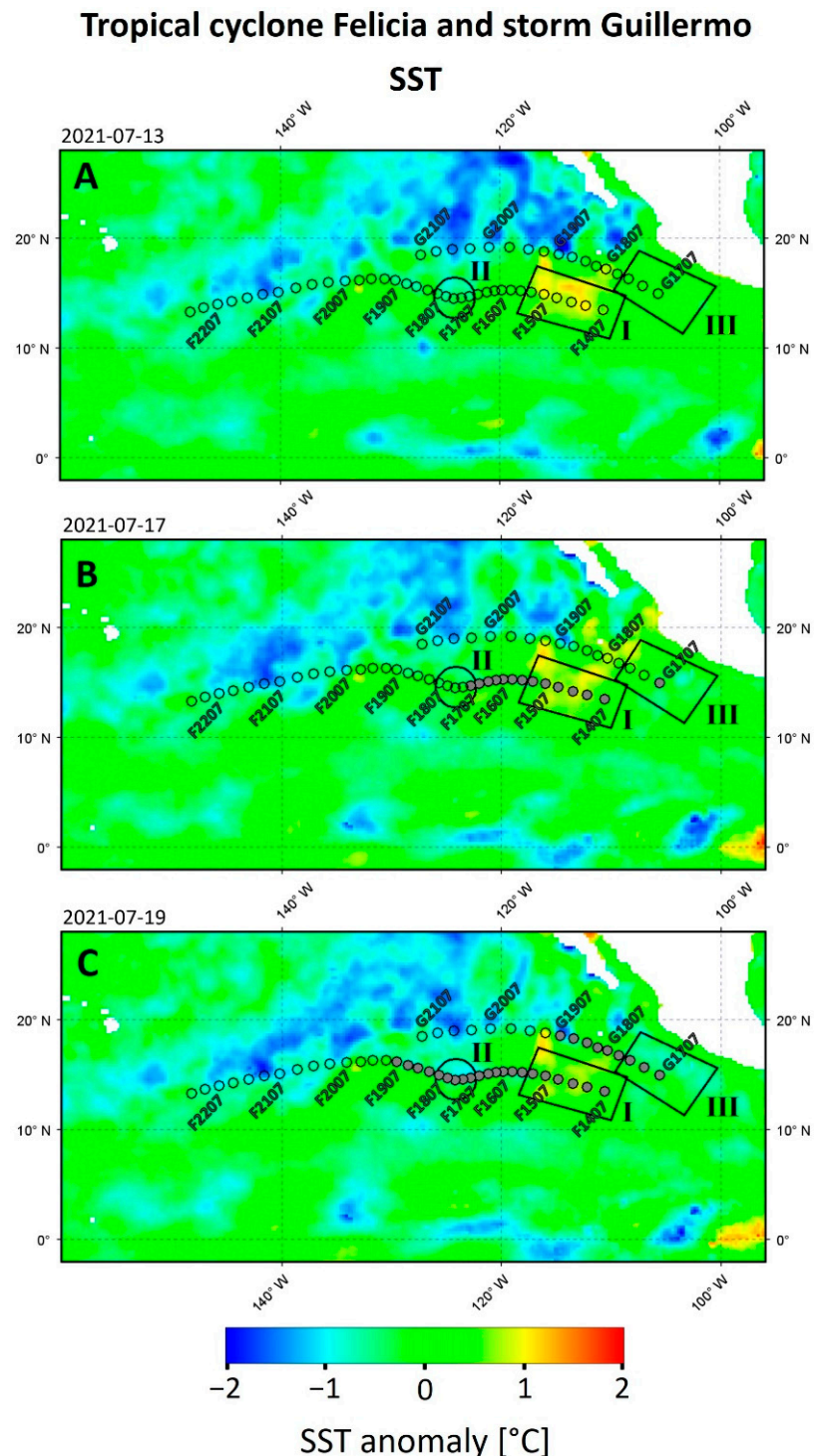


Figure 3. Anomaly maps for SST in the study area of TC Felicia and tropical storm Guillermo for (A) 13 July 2021, (B) 17 July 2021 and (C) 19 July 2021. Anomalies are color-coded as indicated by the color bar. Tracks are marked with circles. Open circles indicate that the storm has not yet passed the position. The labels along the track indicate position of TC Felicia (F) and storm Guillermo (G) on a particular day and month, e.g., F1407 or G1707. The dates of satellite images are given on the top left of each panel. White space indicates areas without data.

2.2. Sea-Surface Temperature

For global daily SST data from 2010 to 2021, we used the product Australian Bureau of Meteorology (ABOM) 0.25° resolution Global Australian Multi-Sensor SST Analysis (GAMSSA) from the Group for High Resolution Sea Surface Temperature (GHRSSST) Level 4. This product is available from the United States National Centers for Environmental Information (NCEI) at: <https://www.ncei.noaa.gov/data/oceans/ghrsst/L4/GLOB/ABOM/GAMSSA/>, accessed on 15 February 2022. We subcategorized the SST data for all defined regions and processed the data with the open-source software SeaDAS (<https://seadas.gsfc.nasa.gov/>, accessed on 13 February 2022, Version 8.1.0). For the days in 2021 where SST was examined, data from 2010 to 2020 for the respective days were taken as long-term average by calculating the mean SST. Changes in SST in 2021 for the regions of interest were expressed as anomalies (in °C) between the SST values observed in 2021 and the long-term average from 2010 to 2020.

2.3. Surface Chlorophyll-a

Satellite-derived concentration data of surface chl-a (as mg m⁻³) were taken as a proxy for phytoplankton biomass to examine the possible responses of the phytoplankton in relation to the two TCs. However, in contrast to SST, remote sensing of surface chl-a is constrained by cloud-free conditions, limiting the use of daily acquired data [20,31]. Hence, surface chl-a data was acquired as a 5-day means of daily satellite images from 2010 to 2021 from the Ocean-Color Climate Change Initiative (OC-CCI) project [32]. The data are distributed by the European Space Agency and are available online (<http://www.esa-oceancolour-cci.org/>, accessed on 16 February 2022). For TC Ida, 5-day means were collected from 4 August to 3 October 2021, and for TC Felicia and tropical storm Guillermo, data were collected from 5 June to 23 September 2021. As for SST, surface chl-a data were subcategorized for the defined regions using the software SeaDAS. Data from 2010 to 2020 were taken as a reference by calculating the long-term mean surface concentration of chl-a for each 5-day period. Changes in surface chl-a in 2021 for the respective regions were expressed as anomalies (in mg m⁻³) compared to average data from 2010 to 2020.

2.4. Argo

Array for Real-Time Geostrophic Oceanography (ARGO) is an international program that uses floats to survey the hydrodynamics of ocean basins [33]. The program provides data consisting of hydrodynamic parameters, that is, temperature, salinity, pressure, and selected floats, including additional sensors for oxygen, nitrate, pH, or chlorophyll-a. The floats record depth profiles of the different parameters from a few hundred to 2000 m up to the surface. We obtained Argo data from the CORIOLIS website (<https://www.coriolis.eu.org/Data-Products/Data-selection>, accessed on 22 February 2022) and analyzed the data with OceanDataView (ODV) [34]. We used Argo data from ascended floats close to the passage of the TC in the respective regions. In the Gulf of Mexico, the Argo floats typically have a record interval of three days, whereas Argo floats in the Pacific ascend every 10 days. The latter limits the available data for the passage of TC Felicia.

To illustrate the storm tracks of the TCs, data for the TC's best track have been downloaded from the National Hurricane Center (NHC) at the National Oceanic and Atmospheric Administration (NOAA), available from the link <https://www.nhc.noaa.gov/gis/> (accessed on 29 June 2022). The best track data are illustrated in Figure 4.

All graphs were plotted with R version 4.1.2 [35] using the “ggplot2” package [36], except for the Argo profiles, which were made with ODV [34]. Anomaly maps for SST and surface chl-a were generated with SeaDAS Version 8.1.0 (<https://seadas.gsfc.nasa.gov/>, accessed on 13 February 2022).

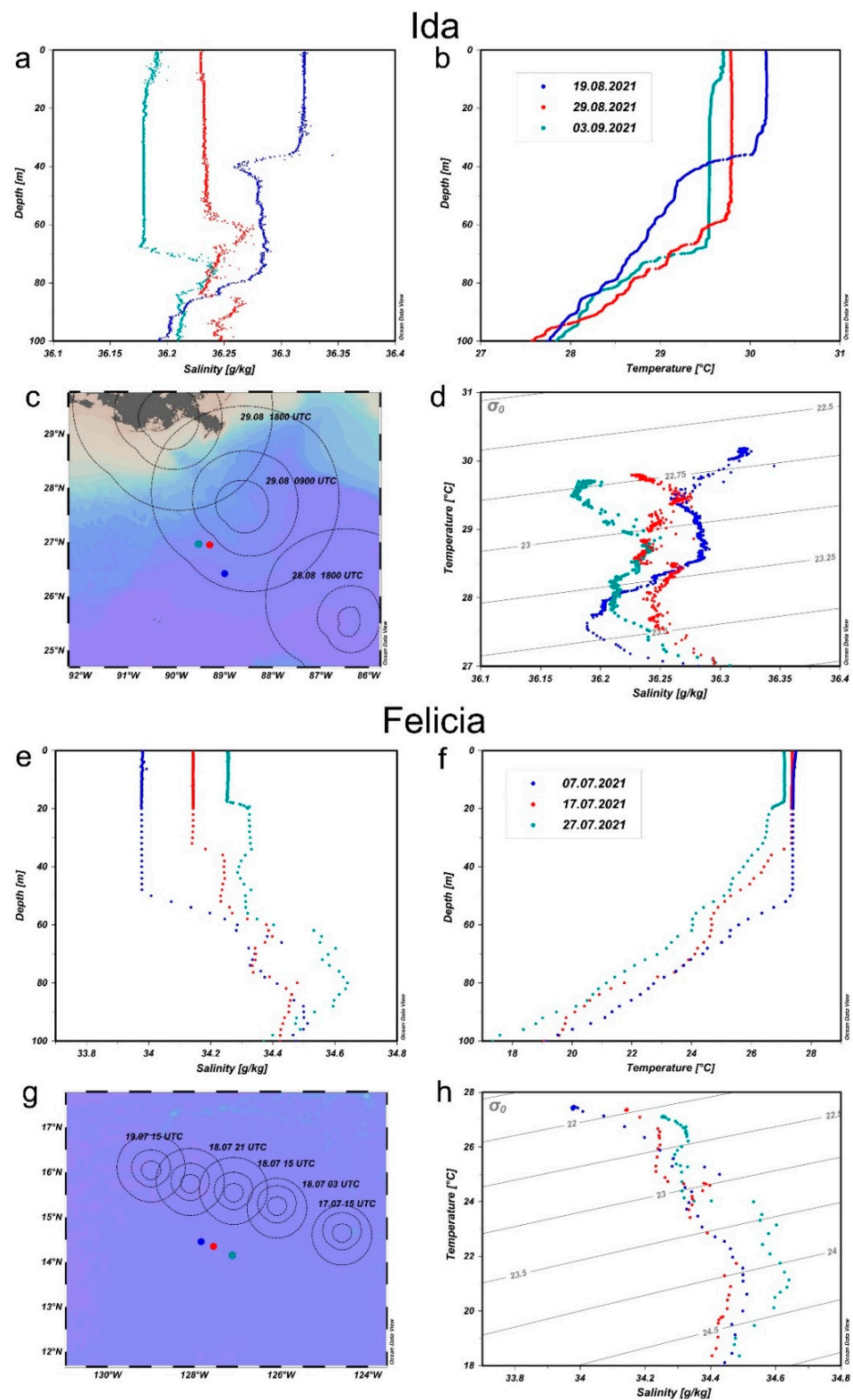


Figure 4. Argo-derived vertical profiles from the Gulf of Mexico for TC Ida (a–d) and from the eastern North Pacific for TC Felicia (e–h). Shown are salinity (a,e) and temperature (b,f) depth profiles, TS diagrams (d,h), and the location of the Argo-floats (c,g), as well as the initial wind radii, which show the maximum extent of the 34 kt, 50 kt, and 64 kt winds in each quadrant of the storm. The date of the measurements is indicated by different colors. Argo numbers are 4903554 for Ida and 5906400 for Felicia.

3. Results

3.1. SST

When TC Ida developed in August 2021, the Caribbean Sea was characterized by SST of 29 °C increasing up to 31 °C toward the Gulf of Mexico (see Figure S1 in the Supplementary Material). The observed SST anomalies vary within the Gulf of Mexico and show warming and cooling sea surfaces after TC Ida (see Figure 1A). Before the passage of Ida, the region HA was about 0.55 °C warmer compared to the reference period (2010–2020), whereas the other regions were around 0.2–0.75 °C colder. For the regions HA, WF, and CB, a cooling of SST after the passage of Ida was observed (Figures 1A and 2). For the same time period, the region (OM) showed an opposite effect and warmed up markedly by over 0.5 °C compared to the reference period (Figures 1A and 2). On 30 August 2021, one day after landfall, the regions OM and WF reached their peaks in warming and cooling, respectively. Five days after landfall, SST returned almost completely to the pre-storm state. Interestingly, the overall SST anomaly in the Gulf of Mexico, considering the entire basin, only slightly changed (see region GoM in Figure 1A).

In the eastern North Pacific, SST was highest north of the equator, with temperatures up to 29 °C in July 2021 (Figure S2 in the Supplementary Material). North of 20° N latitude, water masses were markedly colder (<20 °C), as observed from the remotely-sensed SST in July 2021 (see Figure S2). As shown in Figure 3A, these water masses were approximately −1 °C colder than the 10-year average, which was probably one of the reasons for the abrupt dissipation of both storms. Overall, SST was already variable before Felicia and Guillermo emerged in the eastern North Pacific (Figure 1B). In the regions where Felicia (Region I) and Guillermo formed (Region III), SST was 0.2–0.5 °C warmer than on average, whereas Region II was, on average, 0.25 °C cooler. With and after the development of Felicia and Guillermo, SST markedly decreased in the regions of interest (Figures 1B and 3B,C). By the time Felicia developed on 14 July 2021, SST decreased by −0.25 °C from 13 July to 15 July 2021 in Region I. SST further decreased in the region and was approximately −0.5 °C lower on 28 July 2021 compared to 13 July 2021 (Figure 1B). Hence, there was no recovery of SST to pre-storm conditions within two weeks after the dissipation of Felicia. Although not classified as a TC, the tropical storm Guillermo reduced SST in its place of origin (Region III) by approximately −0.6 °C from 15 July to 19 July 2021, which was the strongest response in SST observed in this study (Figure 1B). As a result, SST was −0.36 °C cooler compared to the 10-year average but then rapidly recovered to pre-storm level by 23 July 2021. Interestingly, when Felicia reached its maximum wind speeds in Region II, the SST response decreased by −0.34 °C, weaker than that after Guillermo's overpass in Region III. SST in Region II recovered within 1 week after the passage TC Felicia (Figure 1B).

3.2. Temperature and Salinity Profiles

Argo profiles of temperature and salinity in the Gulf of Mexico 10 days before, during, and 6 days after the passage of TC Ida are shown in Figure 4. Before Ida's passage, the temperature and salinity were highest in the mixed layer. The TS diagram for Ida (Figure 4d) shows distinct water masses with changes in their hydrodynamic properties with the overpass of TC Ida. A deepening of the mixed-layer depth occurred from around 38 m on 19 August to 59 m on 29 August 2021 and to 68 m on 3 September 2021 (Figure 4a,b).

The passage of Ida resulted in increased subsurface cooling and freshening in the Gulf of Mexico above 68 m. This destratification process was observed during the TC on 29 August and with an even stronger effect on 3 September after the TC passage (Figure 4a,b). Changes in stratification were also observed in the eastern North Pacific regarding TC Felicia. However, the ocean salinity response was opposite due to the higher salinity in the lower water body, which was then mixed with the upper layers. The area of precipitation, and therefore the total flux of freshwater in the region, for TC Felicia was lower compared to TC Ida (see Figure S3 in the Supplementary Material), and thus insufficient to compensate for the increase of salinity due to the mixing with deeper water

masses. An increase in salinity was observed in the upper 60 m of the water columns and led to a surface salinification above 60 m and possibly even above 100 m (Figure 4e). The temperature after the passage of Felicia was lower throughout the water column ($>0.25\text{ }^{\circ}\text{C}$ cooler above 20 m; Figure 4f). However, the general structure and stratification pattern were still pronounced (Figure 4h at around 20 m).

3.3. Surface Chlorophyll-a

The central part of the Gulf of Mexico showed surface chl-a concentrations below 0.1 mg m^{-3} , whereas along the US and Mexican coastline, concentrations increased by more than two orders of magnitude ($>10\text{ mg m}^{-3}$; Figure 5). Similarly, the eastern North Pacific was characterized by low chl-a concentrations ($<0.1\text{ mg m}^{-3}$) and increased considerably toward the Mexican coast (Figure 6). Further, along the equator, high chl-a concentrations were observed, with primary production fueled by nutrient supply from the large upwelling system off Peru.

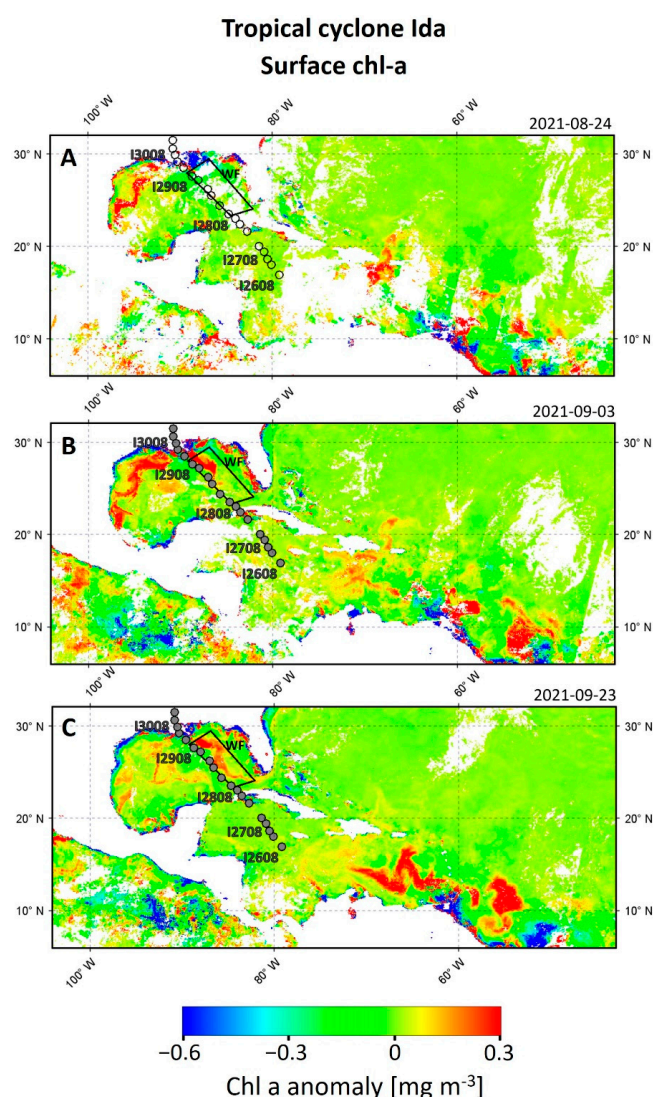


Figure 5. Anomaly maps surface chl-a in the study area of TC Ida for (A) 24 August 2021, (B) 3 September 2021 and (C) 23 September 2021. Anomalies are color-coded as indicated by the color bar. Tracks are marked with circles, where open circles indicate that the storm has not yet passed the position. The labels along the track indicate position of Ida (I) on a particular day and month, e.g., I2608. The dates of the satellite images are given in the top right of each panel. Note that surface chl-a data were obtained as 5-day means (see Methods). White space indicates areas without data.

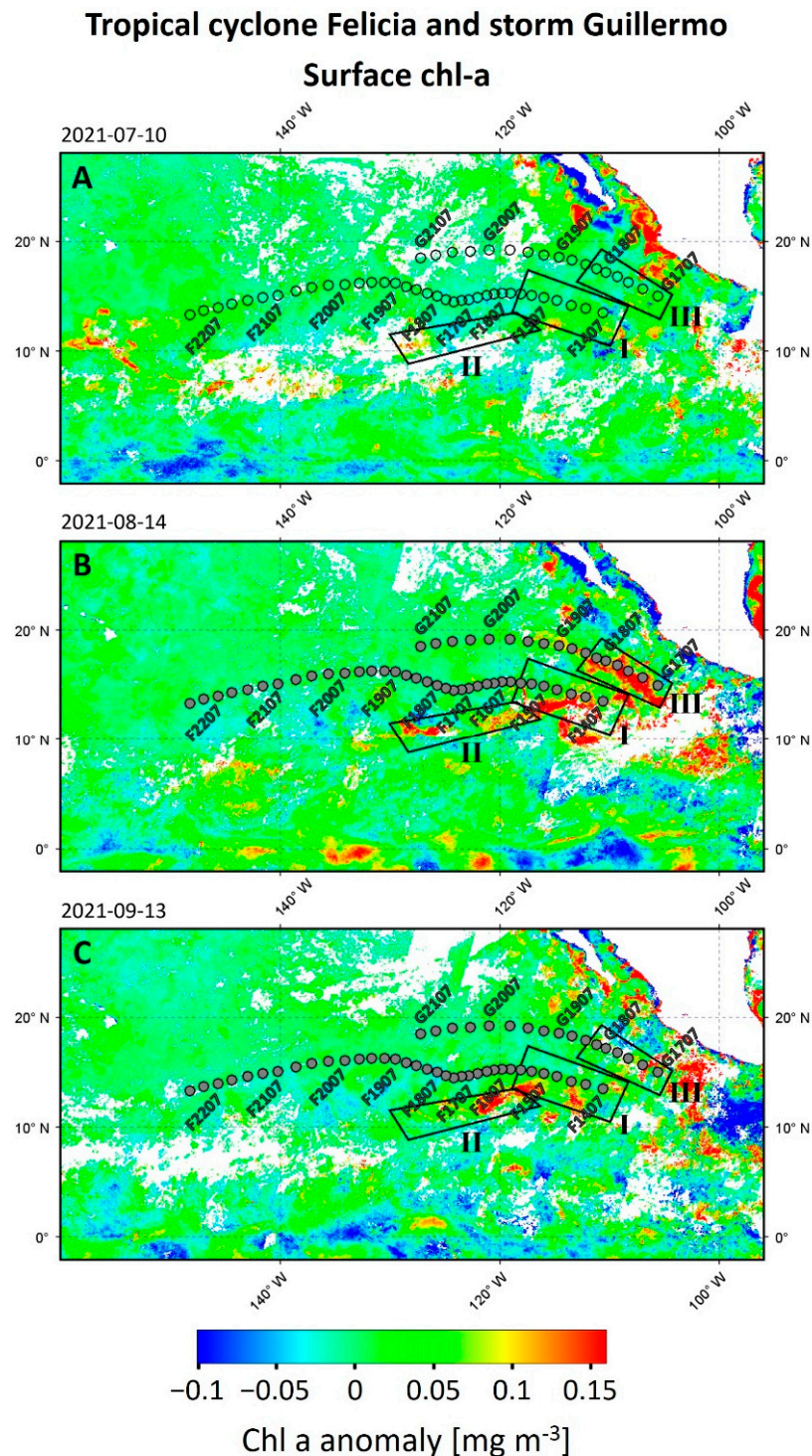


Figure 6. Anomaly maps for surface chl-a in the study area of TC Felicia and tropical storm Guillermo for (A) 10 July 2021, (B) 14 August 2021 and (C) 13 September 2021. Anomalies are color-coded as indicated by the color bar. Tracks are marked with circles. Open circles indicate that the storm has not yet passed the position. The labels along the track indicate position of TC Felicia (F) and storm Guillermo (G) on a particular day and month, e.g., F1407 or G1707. The dates of satellite images are given on the top left of each panel. Note that surface chl-a data were obtained as 5-day means (see Methods). White space indicates areas without data.

All storms investigated in this study caused a notable increase in surface chl-a concentration after their occurrence (see Figure 7). Observed chl-a anomalies remained highly variable in the examined regions, but cloud coverage limited the full assessment of remotely

sensitive chl-a concentrations (cf. anomaly maps in Figures 5 and 6). After the passage of TC Ida, surface chl-a concentrations first decreased but then markedly increased after six days west of Florida on 28 August 2021. Surface chl-a was around 0.19 mg m^{-3} higher than the 10-year average (Figures 5B and 7A). On 8 September 2021, surface chl-a began to decrease but remained slightly higher than on average. For example, satellite images from 23 September 2021, that is, one month after the passage of Ida, showed a region with anomalously high surface chl-a located on the east side of TC Ida's track with a conspicuous filament-like shape (Figure 5C).

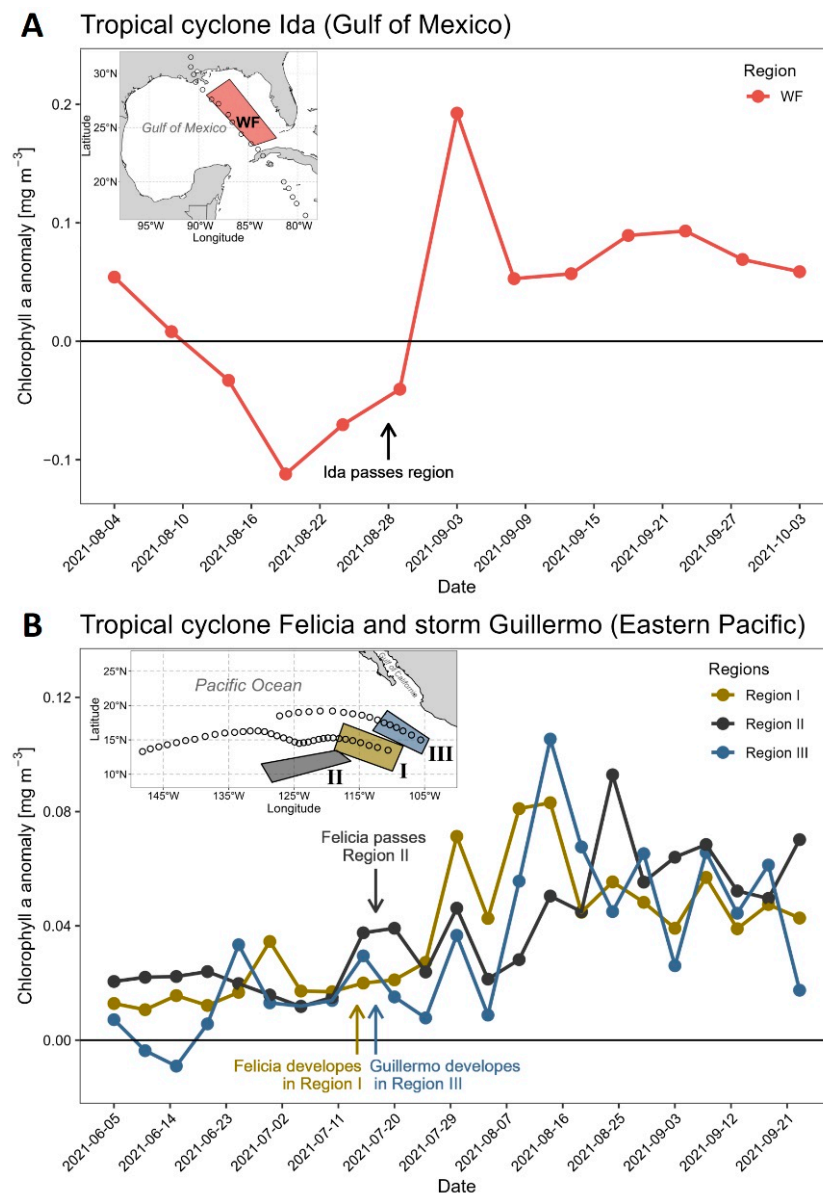


Figure 7. Anomalies in surface chl-a concentration related to TC Ida (A) and TC Felicia and tropical storm Guillermo (B) for the respective regions of interest. Days when storms pass or develop are indicated by arrows and described in the panels.

Compared to Ida, anomalies in surface chl-a concentration caused by TC Felicia and storm Guillermo in the open eastern North Pacific were less pronounced but lasted markedly longer. In the regions of interest, surface chl-a concentrations were already slightly higher than the 10-year average before TC Felicia and Guillermo emerged. However, when the storms developed on 14 and 17 July 2021 in Regions I and III, respectively, a clear increase in surface chl-a was detectable (see Figures 6B and 7B). Surface chl-a

was 0.071 mg m^{-3} higher than the 10-year average from 2010–2020 two weeks after the development of TC Felicia. This increase in chl-a concentration remained detectable by 23 September 2021 (see Figure 7B). For storm Guillermo, surface chl-a increased in Region III, causing an anomaly of $+0.1 \text{ mg m}^{-3}$ on 14 August 2021, that is, one month after storm formation. However, the chl-a concentration decreased and reached pre-storm levels on 23 September 2021. Lastly, in a region south of the track of TC Felicia (see Region II in Figure 6B,C), a considerable increase in surface chl-a up to 0.15 mg m^{-3} was observed, occurring around 24 August 2021 (38 days after Felicia passed along the region).

4. Discussion

4.1. SST

In nearly all regions of interest, the observed changes in SST could be attributed to the appearance of TCs. In the open eastern North Pacific, SST cooling by -0.25 to -0.60 °C was observed as an immediate response to TC Felicia and tropical storm Guillermo, respectively. Cooling of SST after the passage of a TC is a typical response of the upper ocean layer, occurring 1 day after a TC passed over [10]. SST then recovers to pre-storm levels within several days up to several weeks [7,10]. In the Gulf of Mexico, however, strong SST cooling was observed only on the east side of its track immediately after Ida's passage, which needed more than two weeks for complete recovery. For one region offshore Mexico, a warming of SST was observed that started two days before Ida entered the Gulf of Mexico.

The observations in SST before Ida may be caused by the strengthening Loop Current triggered by stronger winds, which transported warmer surface water into the region [11,37]. A coastal boundary effect, together with the Loop Current in the Gulf of Mexico, leads to a different distribution of warm and cold water. Additionally, precipitation plays an important role in the modification of SST. The right front side of a TC is characterized by intense precipitation before landfall [38,39]. This could explain the cooling in the WF and CB regions after the passage of Ida and warming in the OM region. Furthermore, the WF and CB regions are in close proximity to the TC track and are presumably most affected by the high precipitation of Ida (Figure S3). The warming in the OM region could also be a recovery response after the passage of another TC named Grace 6 days prior to TC Ida [40]. The overall relatively small changes in SST relative to the entire Gulf of Mexico (GoM region in Figure 1) are due to the near counterbalancing between warming on the west side and cooling on the east side of the track. For example, the HA region is typically warmer in the summer months compared to other regions in the Gulf of Mexico [41], and our positive SST anomalies (Figure 4a) confirmed a particular warm water mass in region HA in 2021.

The observed SST cooling due to Felicia and Guillermo was between -0.25 and -0.60 °C compared to pre-storm conditions and was markedly weaker than the -1 to -6 °C reported in other studies [3,7,42]. However, the magnitudes of SST cooling related to TCs strongly depend on the characteristics of the underlying water column (e.g., stratification) and the TC itself (wind and translation speeds). For instance, based on a large dataset, Dare and McBride [10] showed that TCs with high wind speed but slow translation speed cause stronger SST cooling. The translation speeds [43,44] of TC Felicia and tropical storm Guillermo were comparable, with $20.6 \pm 5.3 \text{ km h}^{-1}$ ($n = 69$) and $24.7 \pm 4.4 \text{ km h}^{-1}$ ($n = 33$), respectively. Hence, the translation speeds of the cyclones were not the cause of the relatively low SST anomaly.

4.2. Temperature and Salinity Profiles

The propagated surface cooling and modification to stratification induced by the TCs can be described more specifically with the obtained Argo profiles. As shown in Figure 5a,b, we observed a deepening of the thermocline and halocline, as well as a subsurface cold anomaly above and a warm anomaly below 40 m. These results indicate mixing processes and downwelling [7], which were induced by the passage of TC Ida. Background ocean conditions contribute to the upper ocean temperature response. For

example, cold upwelling in an anticyclonic eddy can intensify sea surface cooling [7,45,46]. This background condition with deeper cold-water layers can be observed in the vertical profiles in the Gulf of Mexico. The vertical profiles during TC Ida's passage showed stronger stratification before the cyclone. The surface mixed layer was shallower and had a higher temperature. Afterwards, however, the thermocline deepened due to the strong TC-induced mixing, entrainment processes, and heavy precipitation.

By contrast, Argo profiles in the overpassed region of TC Felicia suggest a more stable stratification and shallower thermocline after the passage of the cyclone. Ocean eddies found in the open eastern North Pacific (Figure S5) may have had an influence on the cooling of SST and salinity in the upper ocean. Ocean eddies can, if they are anticyclonic, increase salinity in the upper ocean [46], as was observed in the region of TC Felicia. The increase in salinity in the water column after the passage of Felicia could be based on the enhanced mixing of surface layers with deeper, saltier, and colder water masses. Furthermore, higher evaporation rates could have exceeded the precipitation rate, which would possibly contribute to the higher salinity after the passage of TC Felicia compared to TC Ida. However, Argo profiles are limited in space and time, and float no. 5906400 ascended to the surface on 17 July 2021 at 1800 (UTC), that is, 20 h prior Felicia's passage. This means that the float probably measured the forefront of the TC and not its center. Further, the next profile was obtained on 27 July 2021, that is, 9 days after the passage. Dare and McBride [10] reported that 44% of observed SST anomalies typically recover within 5 days after the passage of a TC. Thus, the possible cooling of SST induced by Felicia may have recovered before the Argo float ascended again.

Vertical profiles of Argo provide useful information on the physical mechanisms and the magnitude of ocean impacts of TCs, but the spatial and temporal resolution can be limited due to its typical 10-day cycle. For fast-moving TCs, it is challenging to find floats that ascended shortly prior to and after the TC and are in proximity to the overpass region of a TC. Therefore, the details of the responses of the upper ocean to TCs remain largely unavailable. However, the overarching advantages of in situ measurements during extreme high sea states attribute Argo floats to important tools for exploring the impacts of TCs on the upper ocean.

4.3. Surface Chlorophyll-*a*

All TCs investigated in this study caused an increase in surface chl-*a*, but the magnitude and time lag of the responses differed between the Gulf of Mexico and the eastern North Pacific. Increases in surface chl-*a* were generally slower and lasted markedly longer than the response to SST, simply due to the different time scales of the involved biological and physical processes.

For TC Ida in the Gulf of Mexico, a positive response of surface chl-*a* was observed 6 days after the TC passed the West Florida region and was quantified to be 0.19 mg m^{-3} above the 10-year average. Responses related to Felicia and Guillermo at their places of origin were strongly delayed (16 days and 28 days, respectively) and weaker ($+0.071 \text{ mg m}^{-3}$ and $+0.1 \text{ mg m}^{-3}$, respectively). The latest response of surface chl-*a* was found south of Felicia's track, with a positive anomaly of $+0.09 \text{ mg m}^{-3}$ observed 38 days after the passage of Felicia. The long-term delay in response indicates the entrainment of upwelled nutrients toward the surface rather than pre-existing phytoplankton communities. The time lags found for Felicia and Guillermo exceeded those reported in other studies, varying from 3–6 days [17,20–22,47]. Primarily, the long-lasting chl-*a* anomaly can be explained by the presence of a slow-growing community whose growth is further limited by the nutrient iron [48]. For Ida, the chl-*a* response was within 3–6 days, and the determined restoration time matched the 2–3 weeks reported in the literature [15,22,49]. Surface chl-*a* in regions affected by the passage of Felicia and Guillermo decreased only after 4–5 weeks. Reported TC-related increases in surface chl-*a* range from ≤ 0.1 to 3.1 mg m^{-3} [18,20,22,42]. However, several studies [22,42,49] have stressed that such increases in surface chl-*a*, and thus phytoplankton biomass, should not be generalized; instead, the magnitude strongly depends on

ocean preconditions (e.g., nutricline depth) and cyclone properties (e.g., intensity and transit time). Argo-derived profiles of temperature and salinity indicated TC-induced vertical mixing, which could have led to an upward entrainment of nutrients in both study areas; however, available Argo floats scarcely overlapped with the regions of interest. Other studies support the rarity of clear chl-a responses related to TCs. Babin et al. [15], for instance, analyzed phytoplankton blooms induced by 13 TCs between 1998 and 2001 and only for one TC did after-storm chl-a response exceed pre-storm values by more than 0.05 mg m^{-3} . Lin's [42] study on the western North Pacific detected phytoplankton bloom in only two cases out of eleven TCs in 2003. Menkes et al. [22] analyzed satellite data of approximately 1000 TCs that emerged between 1998 and 2007 and of the induced phytoplankton blooms; only around 10% of the surface chl-a responses exceeded 0.1 mg m^{-3} . Thus, the local impact of TC-related increases in surface chl-a responses should be carefully interpreted.

A striking observation in the Gulf of Mexico was the filament-like shape of the phytoplankton bloom located west of Florida. Filaments with higher surface chl-a concentrations were also observed in previous studies and were related to TC-induced ocean eddies carrying coastal phytoplankton blooms toward the open sea [16,17,20,37]. Walker et al. [17] and Yuan et al. [37] described this phenomenon, particularly for the Gulf of Mexico. They detected hurricane-induced eddies as a transport mechanism for a phytoplankton bloom in the Mississippi River plume, carrying it toward the open Gulf of Mexico, where it lasted approximately two weeks. Our study confirms this transport of biomass into the open waters of the Gulf of Mexico. In the absence of hurricane forces, wind-driven surface currents directed westward limit the exposure of the Mississippi River plume to the open gulf, so fluvial nutrients and massive phytoplankton blooms are mainly restricted to the coast [37,50,51]. However, hurricanes have the potential to break these coastal currents and, thus, inject large amounts of fluvial nutrients, organic matter, and phytoplankton into the otherwise rather oligotrophic Gulf of Mexico [37]. Furthermore, the excessive rainfall related to TC Ida probably further enhanced the terrestrial runoff of organic matter and nutrients into rivers and coastal waters, fueling phytoplankton blooms along the coastline.

5. Conclusions

Using remotely-sensed SST and surface chl-a concentrations, as well as Argo-derived vertical profiles of temperature and salinity, we detected the various effects of two TCs and a tropical storm on vertical mixing and primary production in two different regions. TC Felicia and the tropical storm Guillermo both markedly cooled the surface water along their tracks between 0.36 and 0.50 °C, but the observed cooling could not be related to their wind speed. Ida, however, led to cooling along the east side of the track and warming along the west side in each case by 0.50 °C. Based on our findings, we can conclude that the cooling effect of TCs is complicated and not only related to their wind speeds. The TC Ida caused a deepening of the stratification from 38 m to 68 m but the stratification became shallower from 50 m to 20 m after the overpass of the smaller TC Felicia. Data from Argo floats are crucial to understanding the effects on the upper ocean, and more targeted deployments in regions with a high probability of TC overpasses should be considered in the future. This includes biogeochemical Argo floats (<https://biogeochemical-argo.org/>, accessed 1 November 2022) to understand the increase in primary production with overpasses of TCs. For example, we found an extraordinary long-lasting surface chl-a anomaly in the eastern Pacific two months after Felicia and Guillermo passed, which was probably caused by a slow-growing phytoplankton community under a limitation of the nutrient iron. Due to the geophysical setting, by contrast, Ida distributed a pre-existing coastal bloom into the open waters of the Gulf of Mexico.

Supplementary Materials: The following supporting information can be downloaded at: <https://www.mdpi.com/article/10.3390/rs14215520/s1>, Figure S1: remotely-sensed sea-surface temperature (SST, in °C) on 24 August 2021 for the study area of tropical cyclone Ida, including the Gulf of Mexico and the Caribbean Sea. SST values are color-coded as indicated by the color bar on the right.; Figure S2: remotely-sensed sea-surface temperature (SST, in °C) on 11 July 2021 for the study area of tropical

cyclone Felicia and the tropical storm Guillermo. SST values are color-coded as indicated by the color bar on the right.; Figure S3: precipitation rates for (a) TC Felicia and (b) TC Ida. Images provided by JAXA/EORC Tropical Cyclone Database (https://sharaku.eorc.jaxa.jp/TYP_DB/index.html); Figure S4: sea surface heights for TC Ida in the Gulf of Mexico on the 24 and 29 August and 3 September 2021 (A, B, C, respectively). Data provided by Fournier S., Willis J., Killett E., Qu Z. and Zlotnicki V. 2022. SEA_SURFACE_HEIGHT_ALT_GRIDS_L4_2SATS_5DAY_6THDEG_V_JPL2205. Ver. 2205. PO.DAAC, CA, USA. Dataset accessed on (23 October 2022) at <https://doi.org/10.5067/SLREF-CDRV3>; Figure S5: sea surface heights for TC Felicia in the eastern North Pacific on the 10, 20, and 30 July 2021 (A, B, C, respectively). Data provided by Fournier S., Willis J., Killett E., Qu Z. and Zlotnicki V. 2022. SEA_SURFACE_HEIGHT_ALT_GRIDS_L4_2SATS_5DAY_6THDEG_V_JPL2205. Ver. 2205. PO.DAAC, CA, USA. Dataset accessed on (23 October 2022) at <https://doi.org/10.5067/SLREF-CDRV3>.

Author Contributions: Conceptualization, O.W.; methodology, O.W., S.N. and J.J.; visualization, S.N. and J.J.; data curation, S.N. and J.J.; investigation, S.N., J.J. and O.W.; writing and editing, S.N., J.J. and O.W. All authors have read and agreed to the published version of the manuscript.

Funding: This research received no external funding.

Institutional Review Board Statement: Not applicable.

Informed Consent Statement: Not applicable.

Data Availability Statement: Data on sea surface temperature are available at the United States National Centers for Environmental Information (NCEI) at: <https://www.ncei.noaa.gov/data/oceans/ghrsst/L4/GLOB/ABOM/GAMSSA/> (accessed on 17 September 2022). ARGO data are archived on the CORIOLIS website (<https://www.coriolis.eu.org/Data-Products/Data-selection>, accessed on 17 September 2022). Satellite-derived concentration data of surface chlorophyll-a are distributed by the European Space Agency and are available online (<http://www.esa-oceancolour-cci.org/>, accessed on 17 September 2022).

Acknowledgments: We are very thankful to the Australian Bureau of Meteorology, the OceanColor Group, the United States National Centers for Environmental Information, the European Space Agency, and the ARGO Community for assimilation and sharing data. We thank JAXA/EORC Tropical Cyclone Database (https://sharaku.eorc.jaxa.jp/TYP_DB/index.html, accessed 1 November 2022) for providing data on precipitation and images in Figure S3. We thank the Physical Oceanography Distributed Active Archive Center (PO.DAAC) at the Jet Propulsion Laboratory for providing data on sea surface height in Figures S4 and S5.

Conflicts of Interest: The authors declare no conflict of interest.

References

1. Seneviratne, S.I.; Nicholls, N.; Easterling, D.; Goodess, C.M.; Kanae, S.; Kossin, J.; Luo, Y.; Marengo, J.; McInnes, K.; Rahimi, M.; et al. Changes in Climate Extremes and Their Impacts on the Natural Physical Environment. In *Managing the Risks of Extreme Events and Disasters to Advance Climate Change Adaptation. A Special Report of Working Groups I and II of the Intergovernmental Panel on Climate Change*; Field, C.B., Barros, V., Stocker, T.F., Qin, D., Dokken, D.J., Ebi, K.L., Mastrandrea, M.D., Mach, K.J., Plattner, G.-K., Allen, S.K., et al., Eds.; Cambridge University Press: Cambridge, UK; New York, NY, USA, 2012; pp. 109–123.
2. Gray, W.M. Global view of the origin of tropical disturbances and storms. *Mon. Weather Rev.* **1968**, *96*, 669–700. [[CrossRef](#)]
3. Price, J.F. Upper Ocean Response to a Hurricane. *J. Phys. Oceanogr.* **1981**, *11*, 153–175. [[CrossRef](#)]
4. Emanuel, K.A.; DesAutels, C.; Holloway, C.; Korty, R. Environmental Control of Tropical Cyclone Intensity. *J. Atmos. Sci.* **2004**, *61*, 843–858. [[CrossRef](#)]
5. Emanuel, K.A. Thermodynamic control of hurricane intensity. *Nature* **1999**, *401*, 665–669. [[CrossRef](#)]
6. Emanuel, K.A. Tropical Cyclones. *Annu. Rev. Earth Planet. Sci.* **2003**, *31*, 75–104. [[CrossRef](#)]
7. Zhang, H.; He, H.; Zhang, W.-Z.; Tian, D. Upper ocean response to tropical cyclones: A review. *Geosci. Lett.* **2021**, *8*, 1. [[CrossRef](#)]
8. Jacob, S.D.; Shay, L.K.; Mariano, A.J.; Black, P.G. The 3D Oceanic Mixed Layer Response to Hurricane Gilbert. *J. Phys. Oceanogr.* **2000**, *30*, 1407–1429. [[CrossRef](#)]
9. D’Asaro, E.A. The Ocean Boundary Layer below Hurricane Dennis. *J. Phys. Oceanogr.* **2003**, *33*, 561–579. [[CrossRef](#)]
10. Dare, R.A.; McBride, J.L. Sea Surface Temperature Response to Tropical Cyclones. *Mon. Weather Rev.* **2011**, *139*, 3798–3808. [[CrossRef](#)]
11. Shay, L.K.; Goni, G.J.; Black, P.G. Effects of a Warm Oceanic Feature on Hurricane Opal. *Mon. Weather Rev.* **2000**, *128*, 1366–1383. [[CrossRef](#)]

12. Lloyd, I.D.; Vecchi, G.A. Observational Evidence for Oceanic Controls on Hurricane Intensity. *J. Clim.* **2011**, *24*, 1138–1153. [[CrossRef](#)]
13. Balaguru, K.; Chang, P.; Saravanan, R.; Leung, L.R.; Xu, Z.; Li, M.; Hsieh, J.-S. Ocean barrier layers' effect on tropical cyclone intensification. *Proc. Natl. Acad. Sci. USA* **2012**, *109*, 14343–14347. [[CrossRef](#)] [[PubMed](#)]
14. Lin, I.-I.; Wu, C.-C.; Pun, I.-F.; Ko, D.-S. Upper-Ocean Thermal Structure and the Western North Pacific Category 5 Typhoons. Part I: Ocean Features and the Category 5 Typhoons' Intensification. *Mon. Weather Rev.* **2008**, *136*, 3288–3306. [[CrossRef](#)]
15. Babin, S.M.; Carton, J.A.; Dickey, T.D.; Wiggert, J.D. Satellite evidence of hurricane-induced phytoplankton blooms in an oceanic desert. *J. Geophys. Res. Ocean.* **2004**, *109*, C03043. [[CrossRef](#)]
16. Davis, A.; Yan, X.-H. Hurricane forcing on chlorophyll-a concentration off the northeast coast of the U.S. *Geophys. Res. Lett.* **2004**, *31*, L17304. [[CrossRef](#)]
17. Walker, N.D.; Leben, R.R.; Balasubramanian, S. Hurricane-forced upwelling and chlorophyll a enhancement within cold-core cyclones in the Gulf of Mexico. *Geophys. Res. Lett.* **2005**, *32*, L18610. [[CrossRef](#)]
18. Lin, I.; Liu, W.T.; Wu, C.-C.; Wong, G.T.F.; Hu, C.; Chen, Z.; Liang, W.-D.; Yang, Y.; Liu, K.-K. New evidence for enhanced ocean primary production triggered by tropical cyclone. *Geophys. Res. Lett.* **2003**, *30*, 1718. [[CrossRef](#)]
19. Chen, C.-T.A.; Liu, C.-T.; Chuang, W.S.; Yang, Y.J.; Shiah, F.-K.; Tang, T.Y.; Chung, S.W. Enhanced buoyancy and hence upwelling of subsurface Kuroshio waters after a typhoon in the southern East China Sea. *J. Mar. Syst.* **2003**, *42*, 65–79. [[CrossRef](#)]
20. Zheng, G.M.; Tang, D. Offshore and nearshore chlorophyll increases induced by typhoon winds and subsequent terrestrial rainwater runoff. *Mar. Ecol. Prog. Ser.* **2007**, *333*, 61–74. [[CrossRef](#)]
21. Tsuchiya, K.; Kuwahara, V.S.; Hamasaki, K.; Tada, Y.; Ichikawa, T.; Yoshiki, T.; Nakajima, R.; Imai, A.; Shimode, S.; Toda, T. Typhoon-induced response of phytoplankton and bacteria in temperate coastal waters. *Estuar. Coast. Shelf Sci.* **2015**, *167*, 458–465. [[CrossRef](#)]
22. Menkes, C.E.; Lengaigne, M.; Lévy, M.; Ethé, C.; Bopp, L.; Aumont, O.; Vincent, E.; Vialard, J.; Jullien, S. Global impact of tropical cyclones on primary production. *Glob. Biogeochem. Cycles* **2016**, *30*, 767–786. [[CrossRef](#)]
23. Foltz, G.R.; Balaguru, K.; Leung, L.R. A reassessment of the integrated impact of tropical cyclones on surface chlorophyll in the western subtropical North Atlantic. *Geophys. Res. Lett.* **2015**, *42*, 1158–1164. [[CrossRef](#)]
24. Weng, J.; Wang, L.; Luo, J.; Chen, B.; Peng, X.; Gan, Q. A Contrast of the Monsoon-Tropical Cyclone Relationship between the Western and Eastern North Pacific. *Atmosphere* **2022**, *13*, 1465. [[CrossRef](#)]
25. Jin, F.F.; Boucharel, J.; Lin, I.I. Eastern Pacific tropical cyclones intensified by El Niño delivery of subsurface ocean heat. *Nature* **2014**, *516*, 82–85. [[CrossRef](#)]
26. Fu, D.; Chang, P.; Patricola, C.M.; Saravanan, R.; Liu, X.; Beck, H.E. Central American mountains inhibit eastern North Pacific seasonal tropical cyclone activity. *Nat. Commun.* **2021**, *12*, 4422. [[CrossRef](#)] [[PubMed](#)]
27. Holbach, H.M.; Bourassa, M.A. The Effects of Gap-Wind-Induced Vorticity, the Monsoon Trough, and the ITCZ on East Pacific Tropical Cyclogenesis. *Mon. Weather Rev.* **2014**, *142*, 1312–1325. [[CrossRef](#)]
28. Beven, J.L.; Hagen, A.; Berg, R. Tropical Cyclone Report (AL092021): Hurricane IDA; National Hurricane Center. 4 April 2022. Available online: https://www.nhc.noaa.gov/data/tcr/AL092021_Ida.pdf (accessed on 21 June 2022).
29. Cangialosi, J.P. Tropical Cyclone Report (EP062021): Hurricane FELICIA; National Hurricane Center. 9 September 2021. Available online: https://www.nhc.noaa.gov/data/tcr/EP062021_Felicia.pdf (accessed on 15 February 2022).
30. Berg, R. Tropical Cyclone Report (EP072021): Tropical Storm GUILLERMO; National Hurricane Center. 15 August 2021. Available online: https://www.nhc.noaa.gov/data/tcr/EP072021_Guillermo.pdf (accessed on 15 February 2022).
31. Zhao, H.; Shao, J.; Han, G.; Yang, D.; Lv, J. Influence of Typhoon Matsa on Phytoplankton Chlorophyll-a off East China. *PLoS ONE* **2015**, *10*, e0137863. [[CrossRef](#)]
32. Sathyendranath, S.; Brewin, R.J.W.; Brockmann, C.; Brotas, V.; Calton, B.; Chuprin, A.; Cipollini, P.; Couto, A.B.; Dingle, J.; Doerffer, R.; et al. An Ocean-Colour Time Series for Use in Climate Studies: The Experience of the Ocean-Colour Climate Change Initiative (OC-CCI). *Sensors* **2019**, *19*, 4285. [[CrossRef](#)]
33. Roemmich, D.; Johnson, G.C.; Riser, S.; Davis, R.; Gilson, J.; Owens, W.B.; Garzoli, S.L.; Schmid, C.; Ignaszewski, M. The Argo Program. Observing the Global Ocean with Profiling Floats. *Oceanography* **2009**, *22*, 34–43. [[CrossRef](#)]
34. Schlitzer, R. Ocean Data View. 2018. Available online: <https://odv.awi.de> (accessed on 22 February 2022).
35. R Core Team. R: A Language and Environment for Statistical Computing. *R Found. Stat. Comput. Vienna Austria* **2021**.
36. Wickham, H. *Ggplot2: Elegant Graphics for Data Analysis*; Springer: New York, NY, USA, 2016.
37. Yuan, J.; Miller, R.L.; Powell, R.T.; Dagg, M.J. Storm-induced injection of the Mississippi River plume into the open Gulf of Mexico. *Geophys. Res. Lett.* **2004**, *31*, L09312. [[CrossRef](#)]
38. Kimball, S.K. Structure and Evolution of Rainfall in Numerically Simulated Landfalling Hurricanes. *Mon. Weather Rev.* **2008**, *136*, 3822–3847. [[CrossRef](#)]
39. Sun, J.; Vecchi, G.; Soden, B. Sea Surface Salinity Response to Tropical Cyclones Based on Satellite Observations. *Remote Sens.* **2021**, *13*, 420. [[CrossRef](#)]
40. Reinhart, B.J.; Reinhart, A.; Berg, R. Tropical Cyclone Report (AL072021): Hurricane GRACE; National Hurricane Center. 18 February 2022. Available online: https://www.nhc.noaa.gov/data/tcr/AL072021_Grace.pdf (accessed on 18 September 2022).
41. Zavala-Hidalgo, J.; Gallegos-García, A.; Martínez-López, B.; Morey, S.L.; O'Brien, J.J. Seasonal upwelling on the Western and Southern Shelves of the Gulf of Mexico. *Ocean Dyn.* **2006**, *56*, 333–338. [[CrossRef](#)]

42. Lin, I.-I. Typhoon-induced phytoplankton blooms and primary productivity increase in the western North Pacific subtropical ocean. *J. Geophys. Res. Ocean.* **2012**, *117*, C03039. [[CrossRef](#)]
43. Knapp, K.R.; Diamond, H.J.; Kossin, J.P.; Kruk, M.C.; Schreck, C.J. International Best Track Archive for Climate Stewardship (IBTrACS) Project, Version 4. NOAA National Centers for Environmental Information. Available online: <https://doi.org/10.25921/82ty-9e16> (accessed on 29 August 2022).
44. Knapp, K.R.; Kruk, M.C.; Levinson, D.H.; Diamond, H.J.; Neumann, C.J. The International Best Track Archive for Climate Stewardship (IBTrACS): Unifying Tropical Cyclone Data. *Bull. Am. Meteorol. Soc.* **2010**, *91*, 363–376. [[CrossRef](#)]
45. Jaimes, B.; Shay, L.K. Mixed Layer Cooling in Mesoscale Oceanic Eddies during Hurricanes Katrina and Rita. *Mon. Weather Rev.* **2009**, *137*, 4188–4207. [[CrossRef](#)]
46. Liu, S.-S.; Sun, L.; Wu, Q.; Yang, Y.-J. The responses of cyclonic and anticyclonic eddies to typhoon forcing: The vertical temperature-salinity structure changes associated with the horizontal convergence/divergence. *J. Geophys. Res. Ocean.* **2017**, *122*, 4974–4989. [[CrossRef](#)]
47. Byju, P.; Prasanna Kumar, S. Physical and biological response of the Arabian Sea to tropical cyclone Phyan and its implications. *Mar. Environ. Res.* **2011**, *71*, 325–330. [[CrossRef](#)]
48. Pennington, J.T.; Mahoney, K.L.; Kuwahara, V.S.; Kolber, D.D.; Calienes, R.; Chavez, F.P. Primary production in the eastern tropical Pacific: A review. *Prog. Oceanogr.* **2006**, *69*, 285–317. [[CrossRef](#)]
49. Hanshaw, M.N.; Lozier, M.S.; Palter, J.B. Integrated impact of tropical cyclones on sea surface chlorophyll in the North Atlantic. *Geophys. Res. Lett.* **2008**, *35*, L01601. [[CrossRef](#)]
50. Cochrane, J.D.; Kelly, F.J. Low-frequency circulation on the Texas-Louisiana continental shelf. *J. Geophys. Res. Ocean.* **1986**, *91*, 10645–10659. [[CrossRef](#)]
51. Walker, N.D. Satellite assessment of Mississippi River plume variability: Causes and predictability. *Remote Sens. Environ.* **1996**, *58*, 21–35. [[CrossRef](#)]